Combinatorial prospects of nanoparticle mediated immunotherapy of cancer

Silva, C.G. da

5

CO-DELIVERY OF IMMUNOMODULATORS IN BIODEGRADABLE NANOPARTICLES IMPROVES THERAPEUTIC EFFICACY OF CANCER VACCINES

Da Silva, C.G., Camps, M.G.M., Li, T.M.W.Y., Chan, A.B., Ossendorp, F., Cruz L.J.

Biomaterials. 2019 Nov; 220:119417.

Abstract

To improve the efficacy of cancer vaccines we aimed to modulate the suppressive tumor microenvironment. In this study, the potential of intratumoral immune modulation with poly(I:C), Resiquimod (R848) and CCL20 (MIP3α) was explored. Biodegradable polymeric nanoparticles were used as delivery vehicles for slow and sustained release of these drugs in the tumor area and were combined with specific immunotherapy based on therapeutic peptide vaccination in two aggressive murine carcinoma and lymphoma tumor models. Whereas nanoparticle delivery of poly(I:C) or R848 improved therapeutic efficacy, the combination with MIP3α remarkably potentiated the cancer vaccine antitumor effects. The long-term survival increased to 75-100 percent and the progression free survival nearly doubled on mice with established large carcinoma tumors. The potent adjuvant effects were associated with lymphoid and myeloid population alterations in the tumor and tumor-draining lymph node. In addition to a significant influx of macrophages into the tumor, the phenotype of the suppressor tumor-associated macrophages shifted towards an acute inflammatory phenotype in the tumor-draining lymph node. Overall, these data show that therapeutic cancer vaccines can be potentiated by the combined nanoparticle mediated co-delivery of poly(I:C), R848 and MIP3α, which indicates that a more favorable milieu for cancer fighting immune cells is created for T cells induced by therapeutic cancer vaccines.

Keywords: immunotherapy, nanoparticles, therapeutic cancer vaccine, immune modulation, immune adjuvants, multi-drug nanoparticle.

1. INTRODUCTION

Recent breakthroughs and acquired understanding of immune mechanisms are compelling vaccines beyond the prophylactic prevention of cancer into the therapeutic class to treat fully established and advanced cancer [1]. The therapeutic potential was also recently acknowledged by the U.S. Food and Drug Administration (FDA) and European Medicines Agency (EMA) approval of Sipuleucel-T (trade name Provenge), a therapeutic cancer vaccine and a first alternative to chemotherapy for the treatment of metastatic prostate cancer [2]. Moreover, several others cancer vaccines are currently in late stage clinical trials and have demonstrated minimal toxicity in all clinical trials that have been reported to date [3]. Although the target antigens are tumor-associated antigens, that are also expressed in normal tissues, autoimmunity has rarely been reported with the exception of vitiligo induced by some melanoma vaccines [4]. Despite that therapeutic vaccines are showing promise, objective clinical responses in established cancers still remain low. Further refinement of therapeutic vaccines, or the combination treatment with other modalities, could therefore improve responses. For instance, the combination of cancer vaccines with immune checkpoint inhibitors has potential but is also currently being challenged with drawbacks, such as discontinuation due to non-responsiveness, toxicity and acquired resistance to immune check point inhibitors, warranting alternative (immune)therapies that can also address negative immune regulation and immune evasion of tumors [5,6]. Several underlying mechanisms of immune evasion have been implicated thus far, including the installment of an immune suppressed tumor microenvironment characterized by chronic inflammatory and suppressive mediators such as TGFβ, IDO, and IL10 [1]. These factors are produced non-exclusively by cancer cells, regulatory T cells (Tregs), suppressor macrophages and myeloid-derived suppressor cells (MDSCs), and can directly inhibit T cell proliferation and induce T cell senescence or apoptosis [7,8]. There is mounting evidence that immunotherapy with immune adjuvants that activate specific pattern recognition receptors (PRRs), such as Toll-Like Receptors (TLRs), may potentially reduce negative regulation [9]. Agonists that activate specific TLRs can skew the chronic inflamed tumor microenvironment towards an acute inflamed state which is a milieu more favorable for cancer fighting cells [10]. Besides to induce broad acute inflammatory responses, there are also indications that the activity of leukocytes is enhanced and the progression from innate to

adaptive immune responses is elicited [11]. The efficacy of TLR agonists as a monotherapy or adjuvant therapy in cancer has been studied in human clinical trials and ambivalent results have been reported [12,13]. Generally, the activation of the endosomal viral sensing PRRs TLR3, TLR7, TRL8 and TLR9 were reported to induce more tumor regressions in human patients than bacterial sensing PRRs but only imiquimod (i.e. TLR7 agonist) is currently FDA approved for topical application [14]. Upon systemic treatment, the TLR3 agonist Poly (I:C; pIC) has been described to be able to reprogram the tumor microenvironment towards an acute inflammatory state in liver and lung tumors while the TLR7/8 agonist Resiquimod (R848) has been described to block and reverse tumor mediated T cell senescence in advanced leukemia and skin cancers [12,15–17]. While inducing acute inflammation in the tumor microenvironment is an important factor mediating anti-tumor responses, chemokines can be useful mediators capable to attract specific (immune) cells. For instance, Macrophage Inflammatory Protein-3 alpha (MIP3**α**; CCL20) attracts cells expressing CCR6/CD196 often involved in mediating tumor regressions such as found on immature dendritic cells (DCs), (memory) T cells, natural killer (NK) cells and granulocytes [18–22]. Moreover, MIP3**α** has also been described to directly repress the proliferation of myeloid progenitors [23].

Although TLR agonists are powerful immune stimulators, they can induce unwanted cytokine release syndrome which is a major factor limiting the usage of TLR agonists for the treatment of cancer [12]. In other words, a major challenge is restricting rapid systemic distribution and maintain high local confinement of these immune adjuvants to the tumor area to keep unwanted immune side effects at bay. To this end, targeted drug delivery using bio-compatible nanoparticles (NPs) can be used to minimize these side effects and enhance their efficacy due to their slow and sustained release of drugs capabilities [24]. In addition, the potential applications and advantages of NPs over 'free' compounds are recognized features vastly reviewed and currently being studied in many clinical trials [25]. The usage of drug delivery vehicles such as silica NPs, metallic NPs, liposomes, or biodegradable poly(lactic-co-glycolic acid; PLGA) polymers are prime candidates for upcoming platforms for local drug delivery [26,27].

Herein, we report the assembly and in vitro functional characterization and loading of PLGA NPs with pIC, R848 and MIP3**α**, each individually or in combinations, and subsequent in vivo evaluation of each loaded NPs as an adjuvant modality to

improve the efficacy of two distinct synthetic long peptide based therapeutic cancer vaccines. We assessed the activity of our drug-loaded NPs in two aggressive murine models of cancer that are, to some extent, responsive to therapeutic vaccination: TC-1 lung carcinoma and RMA T cell lymphoma. We provide evidence that the two therapeutic cancer vaccines efficacy can be improved by the intratumoral administration of immune adjuvants co-delivered by NPs. In addition, we show that the combined co-delivery of pIC, R848 and MIP3α is superior to any of these immune adjuvants separately. Mechanistically, we report that the NPs impacted lymphoid and myeloid populations in the tumor and in the tumor-draining lymph node. To the best of our knowledge, this is the first study to combine NP mediated delivery of two distinct TLR agonists and a chemokine into a single modality which improves the efficacy of cancer vaccines.

2. MATERIALS AND METHODS

2.1. Materials and reagents

PLGA polymer (lactide/glycolide molar ratio of 48:52 to 52:48) was purchased from Boehringer Ingelheim (Ingelheim am Rhein, Germany). The near infrared (NIR) dye (IR-780 Iodide; CAS 207399-07-3), poly(inosinic:cytidylic acid; CAS 42424-50-0 P0913), polyvinyl alcohol (PVA; CAS 9002-89-5) and dichloromethane (DCM; CAS 75-09-2 CH2CL2 MW 84.93) were purchased from Sigma-Aldrich (Zwijndrecht, The Netherlands). Chloroform (CHCL3 MW 119.38 g/mol) was purchased from Merck (Darmstadt, Germany). Lipid-PEG 2000 (1,2-Distearoyl-sn-Glycero-3-Phosphoethanolamine-N-[Methoxy(Polyethylene glycol)-2000]; powder MW 2805.54) was purchased from Avanti Polar Lipids (AL, USA). R848 from Alexis Biochemicals (Paris, France) and MIP3α (CCL20) from R&D Systems (MN, USA).

2.2. Preparation of PLGA NPs

The PLGA NPs were synthesized in an oil/water emulsion, using a solvent evaporation-extraction method as described previously [28–31]. Briefly, 200 mg of PLGA powder was dissolved in 3 mL of DCM containing 1 mg of NIR dye. Depending on the NP, the following was added: 8 mg of pIC, and/or 4 mg of R848 and/or 250 μg of MIP3α. The prepared solution was then added dropwise to 40 mL of aqueous 2.5% (w/v) PVA and emulsified for 120 s using a sonicator (250 watt; Sonifier 250; Branson, Danbury, USA). Next, the emulsion was gently poured to a beaker previously prepared containing an air-dried film of 20 mg of Lipid-

PEG 2000 dissolved in 0.2 mL of chloroform, homogenized for 60 s by sonication after which the solvents were evaporated overnight at 4 °C on a magnetic stirrer. Following NP collection by ultracentrifugation and lyophilization, the concentration of the NPs constituents was determined by reverse phase high-performance liquid chromatography (RP-HPLC), as described elsewhere [32].

2.3. Physicochemical properties of the NPs

The NPs were characterized for average size, polydispersity index and surface charge (zeta-potential) by dynamic light scattering. Briefly, 50 µg of NP sample in 1 mL of ultrapure MilliQ H2O were measured for size using a Zetasizer (Nano ZS, Malvern Ltd., UK) and a similar sample was analyzed for surface charge by laser Doppler electrophoresis on the same device.

2.4. Mice strains

C57BL/6 (H-2b haplotype) and 8 to 12 weeks of age female mice were purchased from Envigo (Horst, The Netherlands). The mice were housed at the animal facility of Leiden University Medical Center under specific pathogen free conditions. All animal experiments were approved by the Dutch Central Committee on Animal Experimentation and were strictly conducted according to the Dutch animal welfare law.

2.5. Cell lines

The murine tumor cell line TC-1 (a kind gift from T.C. Wu, Johns Hopkins University, Baltimore, MD, USA) was generated by retroviral transduction of lung fibroblasts of C57BL/6 origin, to express the HPV16 E6 and E7 genes and the activated human c-Ha-ras oncogene [33]. RMA is a Rauscher virus-induced T lymphoma line of C57BL/6 (H-2b) origin [34]. The D1 cell line is an immature splenic DC line with characteristics of that of bone marrow derived DCs [35]. The TC-1 and D1 cell lines were cultured as described previously [36]. The RMA cell line was cultured in IMDM medium (Lonza, Verviers, Belgium) containing 8% heat-inactivated fetal calf serum (FCS; Greiner bio-one, Alphen a/d Rijn, The Netherlands), penicillin (50 µg/mL; Gibco, Paisley, Scotland), streptomycin (50 µg/mL; Gibco), L-glutamine (2 mM; Gibco) and β-mercaptoethanol (20 µM; Sigma, Saint Louis, USA). The expression of RMA MHC class I H-2Kb/Db was verified before in-vivo experiments (Supplemental Figure S1). All the above described cell lines were incubated at 37° C in 5% CO2 and 100% humidity and routinely screened for Mycoplasma and rodent viruses.

2.6. Intracellular uptake of NPs and immunostaining

The intracellular uptake of NPs was determined by incubating either 10 µg/mL or 20 µg/mL of NPs containing NIR dye (~ 800 nm) with $1x10^4$ D1 cells for 1 hour, 2 hours or 4 hours. After thorough washing to remove unbound NPs the cells were fixed and stained with To-pro 3 iodide (642/661 ~700 nm; Invitrogen; Eugene, USA) to enable cell count. Finally, the NIR dye signal was scanned using an Odyssey scanner infrared imaging system (LI-COR). Immunostaining detected by fluorescence microscopy was determined by incubating 20 µg/mL of NPs containing NIR dye with D1 cells in the chambers of a glass culture slide (FALCON, NY, USA) for 48 hours. After washing and fixation, the cells were stained with anti-I-A/I-E-FITC (clone 2G9, BD Bioscience) for membrane visualization, washed again with PBS and mounted with VectaShield antifade mounting medium with DAPI to stain nuclei (Vector Laboratories, CA, USA). Digital images were acquired using a Leica DM6B microscope.

2.7. Activation and maturation of DCs

The upregulation of CD40, CD80 and CD86 on D1 cells and the production of IL-12 in the supernatant were used as indicators of DC activation and maturation upon co-culture with NPs. Briefly, $5x10^4$ D1 cells were co-cultured with NPs for 48 hours at 37° C in 5% CO2 and 100% humidity. The NP concentrations were matched upon pIC, R848 or PLGA concentration where applicable. The CD86 expression was analyzed with anti-CD86-APC (clone GL1, eBioscience) on an LSR-II laser flow cytometer controlled by CELLQuest software v. 3.0 (Becton Dickinson, Franklin Lakes, USA) and analyzed with FlowJo LLC v. 10 software (Tree Star, USA).). The interleukin IL12 was detected using a standard sandwich ELISA with purified anti-mouse IL12/IL23 p40 (clone C15.6, Biolegend) and biotin-labelled anti-mouse IL12/IL23p40 antibodies (clone C17.8, Biolegend). The plates were read at 450 nm using a Bio-rad 680 microplate reader (Bio-rad Laboratories).

2.8. Blood analysis

The presence of antigen-specific T cells in the blood of TC-1 bearing mice was determined by collecting 50 µL of blood though the caudal vein at day 16. After removal of red blood cells by lysis, the cells were stained with anti-CD8α-PE (clone 53-6.7, eBioscience), anti-CD3-eFluor 450 (clone 17A2, eBioscience) and the APC labeled HPV16 E749-57 (RAHYNIVTF) MHC class I (H-2Db) tetramer.

Finally, the cells were subjected to flow cytometry measurements on an LSR-II laser flow cytometer controlled by CELLQuest software v. 3.0 (Becton Dickinson) and the data analyzed with FlowJo LLC v. 10 software (Tree Star).

2.9. Tumor treatments and vaccinations

Mice were inoculated with $1x10^5$ TC-1 or $1x10^3$ RMA cells in 0.2 mL PBS in the right flank. The TC-1 tumor bearing mice were vaccinated once in the contralateral left flank at day 8 (when the tumors were established and palpable). The TC-1 vaccine consisted of an emulsion of human papillomavirus type 16 E7 43-70 synthetic long peptide (500μM/mouse; sequence GQAEPDRAHYNIVTFCCKCDSTLRLCV that includes both a CD4 (underlined) and a CD8 epitope (double underlined) [37]) together with adjuvant TLR9 agonist CpG (Invivogen, San Diego, USA; 5 nmol/mouse) in 50% (v/v) of Adjuvant Incomplete Freund (IFA; Becton, Dickinson and Company, MD, USA) and sterile PBS administrated in a 100 μL depot subcutaneously. The RMA tumor bearing mice were vaccinated once at day 10 (when the tumors were established and palpable). The RMA vaccine consisted of a mixture of Rauscher mouse leukemia virus (MuLV) synthetic long peptides coding for the Gag-encoded CD8 epitope (50 nM/mouse; sequence CCLCLTVFL) and the Env-encoded CD4 epitope (20 nM/mouse; sequence EPLTSLTPRCNTAWNRLKL) together with adjuvant TLR9 agonist CpG (Invivogen; 5 nmol/mouse) and sterile PBS injected in a 30 μL depot intradermally in the base of the tail. The intratumoral injections of the NPs (30 μL) on the specified mice, were administrated on the same day as the vaccination day (day 8 for TC-1 and day 10 for RMA) and then once more 10 days after. The NPs were dissolved in sterile PBS and the concentration matched between the groups on pIC concentration, otherwise on R848 or on MIP3α. The concentration of the empty NP was matched on the average PLGA weight of all the groups tested. The reference NP used was the NP containing all three immune adjuvants, the concentration per administration was: pIC 2.5 mg/Kg (50 μg), R848 720 μg/Kg (14.4 μg), and MIP3α 155 μg/Kg (3.1 μg). The surviving mice were re-challenged with a second tumor inoculation of cancer cells on the back at day 120 to determine the development of immunological memory against cancer epitopes. Tumor dimensions were measured every other day with a standard caliper and the volume was calculated by multiplying the tumor diameters in all three dimensions. The maximal allowed tumor volume was 2,000 mm3; after this point, mice were sacrificed, which formed the basis for the Kaplan-Meier survival curves.

2.10. Tumor and lymph node analysis

The tumor and the tumor-draining lymph nodes were analyzed ex vivo by sacrificing the mice and resecting the organs at day 18 (mice were treated as per described above). The resected tumors were mechanically broken up into small pieces using sterile scissors and forceps and then incubated with Liberase TL (Roche, Mannheim, Germany) in serum-free IMDM medium for 15 minutes at 37 °C. Single cell suspensions were acquired from the tumors and lymph nodes by gently grinding the tumor fragments through a 70 μm cell strainer (Falcon, NY, USA). Cells were then equally divided to be stained with two distinct antibody panels. The lymphoid markers panel contained the viability dye 7-AAD (Invitrogen) and the following antibodies against cell surface markers: anti-CD45.2-APC eFluor 780 (clone 104, eBioscience); anti-CD3-eFluor 450 (clone 17A2, eBioscience); anti-CD4-Brilliant Violet 605 (clone RM4-5, Biologend); anti-CD8α-APC-R700 (clone 53-6.7, BD Bioscience); anti-CD25-APC (clone PC61.5, eBioscience); anti-CD49b-PE (clone DX5, BD Bioscience) and anti-CD44-FITC (clone IM7, eBioscience). The myeloid markers panel contained the viability dye 7-AAD (Invitrogen) and the following antibodies against cell surface markers: anti-CD45.2-FITC (clone 104, BD Bioscience); anti-CD11b-eFluor 450 (clone M1/70, eBioscience); anti-F4/80-PE (clone BM8, eBioscience); anti-Ly6G-AlexaFluor 700 (clone 1A8, Biolegend); anti-Ly6C-Brillian Violet 605 (clone HK1.4, Biolegend), and anti-CD11c-APC-eFluor 780 (clone N418, eBioscience). The expression of the cell markers was analyzed on an LSR-II laser flow cytometer controlled by CELLQuest software v. 3.0 (Becton Dickinson) and the data analyzed with FlowJo LLC v. 10 software (Tree Star).

2.11. RMA MHC class I H-2Kb/Db expression

The MHC class I H-2Kb/Db expression was determined by staining $1x10^5$ RMA and $1x10^5$ CT-26 (negative control, Balb/c genetic background) cells with anti-H-2Db-biotin (clone 28-14-8, BD Bioscience) and on a separate well with anti-H-2Kb (obtained via isolation of serum IgG). The Streptavidin-APC conjugate (BD Bioscience) and anti-IgG-Alexa647 (A21237, Life Technologies) secondary antibody were used for signal detection. Finally, after washing, the cells analyzed on an LSR-II laser flow cytometer controlled by CELLQuest software v. 3.0 (Becton Dickinson) and the data analyzed with FlowJo LLC v. 10 software (Tree Star).

2.12. Data and statistical analysis

Statistical analysis was performed using GraphPad Prism v. 7.0 software (GraphPad Software, La Jolla, USA). Data are represented as mean values ± SD unless stated otherwise. Blood, tumor and lymph nodes cell analysis results were compared on a fixed day between mouse groups and statistical significance was determined by using an unpaired, non-parametric, two-tailed Mann-Whitney U test. Survival curves were compared using the Log-rank (Mantel-Cox) test unless stated otherwise. Statistical differences were considered significant at $p < 0.05$ and presented as: * $p < 0.05$, ** $p < 0.01$, *** $p < 0.001$.

3. RESULTS

3.1. Preparation, physicochemical properties and in vitro evaluation of NPs

Here, we prepared a distinct PLGA NP formulation using a solvent evaporation-extraction method using the biodegradable polymer PLGA. For the current study, we loaded the NPs with the immune adjuvants pIC, R848 and the chemokine MIP3**α**, either separately or in combinations (Table 1). Each batch, including the empty (control) NPs, were functionalized with surface PEGylation (PEG) and contained a NIR dye. The PLGA NPs were characterized to ascertain their size and surface charge. The size of NPs was found to range between 140 and 270 nm (Table 1, Figure S2A), depending on the encapsulated content, and the surface charge was negative ranging from -18 to -29 mV (Table 1, Figure S2B).

Table 1. Physicochemical characterization of PLGA NPs

				Loading capacity (% w/w)			
Samples	Diameter	ζ Potential (mV)	PDI	NIR	pIC	R848	MIP3α
NP(NIR)-PEG Annotated as: NP(empty)	196.5 ± 41.8	-25.2 ± 11.4	0.463	64.1	-	-	-
NP(NIR+MIP3α)-PEG Annotated as: NP(MIP3α)	141.4 ± 30.6	-22.5 ± 7.7	0.04	61.6	-	-	64.9
NP(NIR+R848)-PEG Annotated as: NP(R848)	149.4 ± 32.1	-18.1 ± 5.8	0.066	62.7	-	56.3	-
NP(NIR+pIC)-PEG Annotated as: NP(pIC)	149.7 ± 29.2	-21.1 ± 7.3	0.032	57.8	44.6	-	-
NP(NIR+pIC+R848)-PEG Annotated as: NP(pIC+R848)	157.7 ± 37.7	-26.0 ± 7.5	0.08	63.9	47.0	56.4	-
NP(NIR+pIC+R848+MIP3α) -PEG Annotated as: NP(pIC+R848+MIP3α)	268.5 ± 48.2	-29.4 ± 5.1	0.457	59.3 ± 7.3	43.1 ± 9.5	48.0 ± 21.0	62.4 ± 4.9

Physicochemical characterization of the PLGA-PEG NPs containing different immune adjuvants. The PLGA NPs were characterized by dynamic light scattering and zeta potential measurements. PLGA NPs size and zeta potential data represent the mean value ± SD of 10 readings of one representative batch. The loading capacity of the NIR dye was measured by fluorescence method. The loading capacity of pIC, R848 and MIP3α was determined by RP-HPLC analysis. The loading capacity data represent the average value ± SD of batch variation where applicable.

3.1.1. Cellular uptake of NPs

Efficient uptake of the NPs by cells is required for the delivery of the immune adjuvants to their intracellular targets. We incubated DCs with NPs containing NIR dye (at 10 μg/mL and at 20 μg/mL of NPs respectively) for 1, 2 and 4 hours and quantified the relative uptake (Figure 1A). For both concentrations, the uptake increased over time. To corroborate that the signal emanated from inside the cells, DCs were incubated with NPs and analyzed by fluorescence microscopy (Figure 1B). Indeed, the NIR dye signal (green) from the NPs was found to originate within the cells, indicating that these NPs were successfully taken up by DCs.

3.1.2. NPs enhance DC activation and IL-12 production

The activation of the endosomal TLR3 and TLR7/8 enhances the expression of CD40, CD80 and CD86 on DCs and stimulates the production of IL-12. Therefore, we measured these parameters to determine whether pIC and R848 remained active after loading in NPs. To this end, all the distinct NP batches were independently incubated with DCs. The NP(pIC), NP(R848), NP(pIC+R848) and NP(pIC+R848+MIP3α), but not NP(empty) or NP(MIP3α), were found to efficiently enhance the expression of CD40, CD80 and CD86 (Figure 1C) and induce the production of IL-12 (Figure 1D). These results indicate that pIC and R848 remained active after loading in NPs.

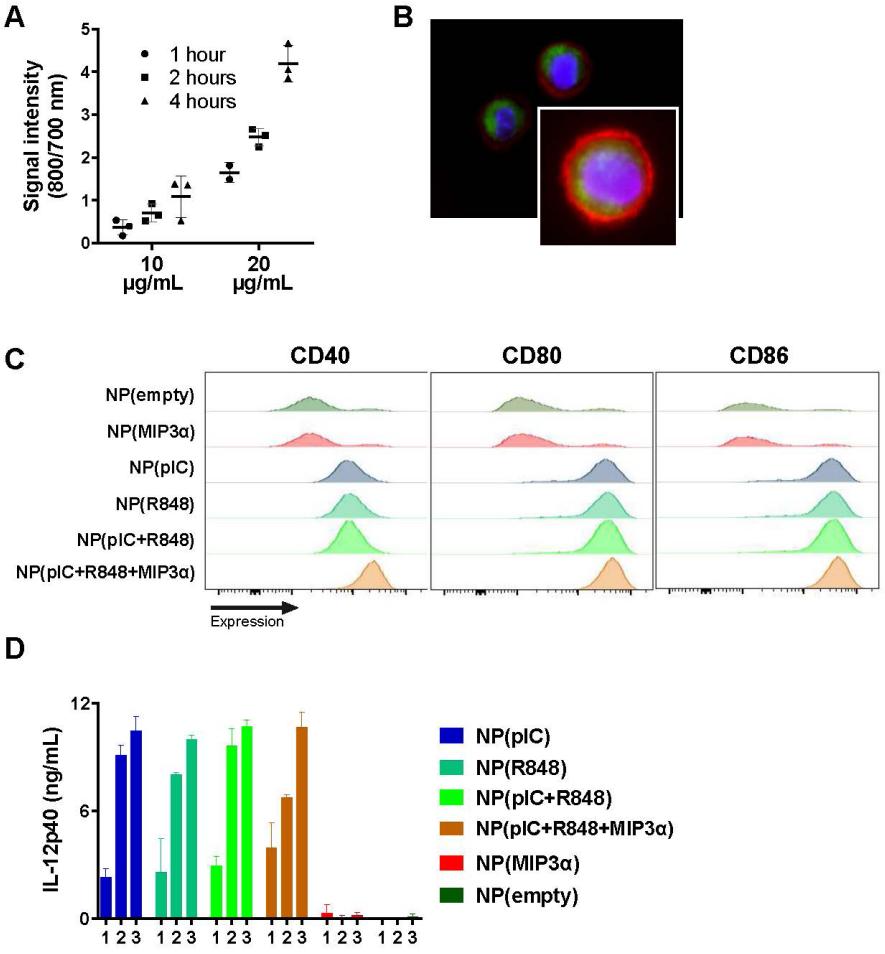

Figure 1. In vitro DC cellular uptake and activation by PLGA NPs loaded with different immune stimulatory compounds

A) Uptake of NPs containing NIR dye (800 nm) by DCs (To-pro 3 iodide; 700 nm) over the times indicated. n = 3 from one representative experiment. **B)** Uptake of NPs by DCs after 2 hours of incubation, shown by fluorescence microscopy. Red: cell membrane; purple: cell nucleus; green: NIR dye. **C)** Activation of DCs measured by CD40, CD80 and CD86

expression upon 48 hours incubation with NP(empty), NP(MIP3α), NP(pIC), NP(R848), NP(pIC+R848) and NP(pIC+R848+MIP3α). The cells were pooled from n = 3 from each condition, one representative out of three independent experiments. D) Activation of DCs measured by the secretion of IL-12p40 upon 48 hours incubation with NP(empty), NP(MIP3α), NP(pIC), NP(R848), NP(pIC+R848) and NP(pIC+R848+MIP3α). n = 3 from one representative out of three independent experiments. Concentrations 1: 1.3 μg/mL; 2: 2.5 μg/mL; 3: 5 μg/mL.

3.2. Co-delivery of immune adjuvants pIC and R848 by NPs improves the survival of vaccinated mice

TC-1 tumor bearing mice were vaccinated subcutaneously in the contralateral flank at day 8 post tumor inoculation with a therapeutic synthetic long peptide vaccine containing both CD4 and CD8 epitopes against the HPV E7 protein that is expressed by TC-1 cells. At the same time, the tumors were treated with an intratumoral injection with NPs at day 8 and at day 18 (Figure 2A). All the vaccinated mice displayed strong tumor mass regressions that started approximately at day 16 and most tumors became undetectable at day 30 (Figure 2B). However, mice that were only vaccinated experienced tumor relapses rapidly approximately 8-10 days after. The survival of mice improved significantly when vaccination treatment was combined with intratumoral injections of NP(pIC) or with NP(R848), respectively (Figure 2C). The survival of mice vaccinated and treated with intratumoral injections of NP(empty) improved but not significantly. To determine whether the surviving mice developed functional memory T cells against cancer epitopes, we re-challenged the mice again with TC-1 cancer cells. We observed that all the mice were able to clear the new tumor without additional treatments (Figure S3A). We also analyzed the blood of tumor bearing mice after vaccination and intratumoral administration of NPs at day 16 and determined the percentages of circulating CD3+, CD8+ and cancer antigen-specific CD8+ T cells.

We observed that the percentage of CD3+ nor CD8+ T cells was affected by the intratumoral NP treatments with the exception of mice treated with NP(R848) that displayed a small, but significant, decrease of CD8+ T cells in blood compared to vaccinated only mice (Figure S4A). All the vaccinated mice shown detectable cancer specific T cells in blood. However, mice that also were treated with intratumoral injections with NP(pIC) displayed higher percentages of cancer antigen-specific CD8+ T cells, but this difference was not statistically significant. Furthermore, all the mice whose tumors had been eradicated, also rejected a tumor re-challenge at day 100, which indicates development of functional immunological memory against tumor antigens and blood analysis at day 110 revealed the presence of high levels of cancer specific T cells in blood (Figure S3B). These results indicate that either NP(pIC) or NP(R848) independently improved the survival of vaccinated mice significantly.

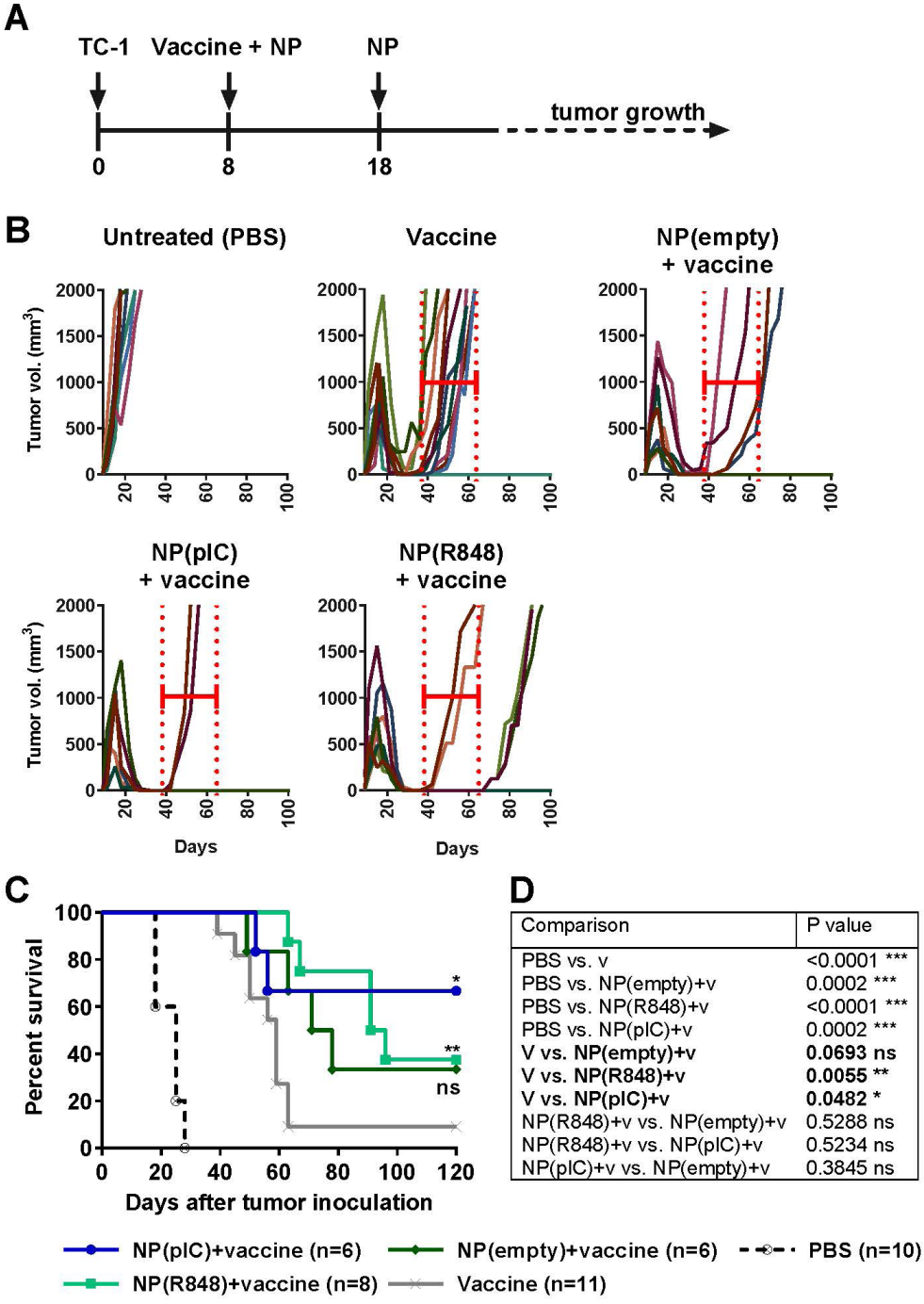

Comparison	P value
PBS vs. v	<0.0001 ***
PBS vs. NP(empty)+v	0.0002 ***
PBS vs. NP(R848)+v	<0.0001 ***
PBS vs. NP(pIC)+v	0.0002 ***
V vs. NP(empty)+v	**0.0693 ns**
V vs. NP(R848)+v	**0.0055 ** **
V vs. NP(pIC)+v	**0.0482 * **
NP(R848)+v vs. NP(empty)+v	0.5288 ns
NP(R848)+v vs. NP(pIC)+v	0.5234 ns
NP(pIC)+v vs. NP(empty)+v	0.3845 ns

Figure 2. Co-delivery of immune adjuvants pIC and R848 by NPs improves the survival of vaccinated mice

A) Schematic diagram of the TC-1 murine model experiment (C57BL/6 mice; n=8 per group, on average), showing inoculation and treatment days. TC-1 tumor bearing mice were vaccinated subcutaneously in the contralateral flank at day 8 post tumor inoculation with a therapeutic synthetic long peptide vaccine containing both CD4 and CD8 epitopes against the HPV E7 protein that is expressed by TC-1 cells. At the same time, the tumors were treated with an intratumoral injection with NPs at day 8 and at day 18. **B)** Tumor growth data from day 0 to day 100 for the PBS (control) group and five treatment groups (vaccine only, vaccine plus empty NPs, vaccine plus R848 and vaccine plus pIC). **C)** Kaplan-Meier survival plots (PBS, vaccine only and NP(pIC+R848) groups data were pooled from two separate experiments), depicting progression-free survival and percent overall survival of vaccinated mice and also treated with NP(empty), NP(pIC) or NP(R848). D) Summary showing the P values for the pairwise comparisons of survival curves. Survival curves were compared using the log-rank test. Statistical differences were considered significant at * $p = < 0.05$; ** $p = < 0.01$; *** $p < 0.001$. Abbreviations: ns: not (statistically) significant; V: Vaccine.

3.3. Co-delivery of MIP3α, in addition to immune adjuvants pIC and R848, improves survival and nearly doubles progression-free survival

Next, we determined whether the survival of vaccinated mice could be further improved by the combination of pIC and R848 and/or chemokine MIP3**α**. To this end, TC-1 tumor bearing mice were vaccinated at day 8 post tumor inoculation as described previously and treated with an intratumoral injection of NPs at day 8 and at day 18 (Figure 3A). We observed that the survival of mice vaccinated and treated with intratumoral injections of NP(MIP3**α**) improved but not significantly (Figure 3B & 3C). On the other hand, the survival of mice vaccinated and treated with intratumoral injections of NP(pIC+R848) or NP(pIC+R848+MIP3**α**) was enhanced significantly. Moreover, the progression-free survival time was found to nearly double compared to either modality (Figure 3B, depicted in the red-dotted lines). To determine whether the surviving mice developed functional memory T cells against cancer epitopes, we re-challenged the mice again with TC-1 cancer cells. We observed that all the mice were able to clear the new tumor without additional treatments (Figure S3A). We also analyzed the blood of tumor bearing mice after vaccination and intratumoral administration of NPs at day 16 and determined the percentages of circulating CD3+, CD8+ and cancer antigen-specific CD8+ T cells. We observed that the percentage of CD3+ nor CD8+ T cells was affected

by the intratumoral NP treatments (Figure S4B). All the vaccinated mice shown detectable cancer specific T cells in blood. However, mice that also were treated with intratumoral injections with NP(pIC+R848) or NP(pIC+R848+MIP3α) displayed higher percentages of cancer antigen-specific CD8+ T cells, but this difference was not statistically significant (Figure S4B). Furthermore, all the mice whose tumors had been eradicated, also rejected a tumor re-challenge at day 100, which indicates development of functional immunological memory against tumor antigens and blood analysis at day 110 revealed the presence of high levels of cancer specific T cells in blood (Figure S3C). These results indicate that the chemokine NP(MIP3α) by itself could not improve the survival of vaccinated mice significantly. However, the combination of the immune adjuvants pIC and R848 improved the overall survival significantly, while the combination of pIC, R848 and MIP3α not only improved the survival of vaccinated mice up to 75%, it nearly doubled the mice progression-free survival time.

Figure 3. Co-delivery of MIP3α, in addition to immune adjuvants pIC and R848, improves survival and nearly doubles progression-free survival >

A) Schematic diagram of the TC-1 murine model experiment (C57BL/6 mice; n=8 per group, on average), showing inoculation and treatment days. TC-1 tumor bearing mice were vaccinated subcutaneously in the contralateral flank at day 8 post tumor inoculation with a therapeutic synthetic long peptide vaccine containing both CD4 and CD8 epitopes against the HPV E7 protein that is expressed by TC-1 cells. At the same time, the tumors were treated with an intratumoral injection with NPs at day 8 and at day 18. B) Tumor growth data from day 0 to day 100 for the PBS (control) group and four treatment groups (vaccine only, vaccine plus MIP3α, vaccine plus pIC and R848 combined, and vaccine plus pIC, R848 and MIP3α combined). The red-dotted lines depict the different progression-free survival times. C) Kaplan-Meier survival plots depicting progression-free survival and percent overall survival of vaccinated mice and also treated with NP(MIP3α) or NP(pIC+R848+MIP3α). D) Summary showing the P values for the pairwise comparisons of survival curves. Survival curves were compared using the log-rank test. Statistical differences were considered significant at * $p = < 0.05$; ** $p = < 0.01$; *** $p < 0.001$. Abbreviations: ns: not (statistically) significant; V: Vaccine

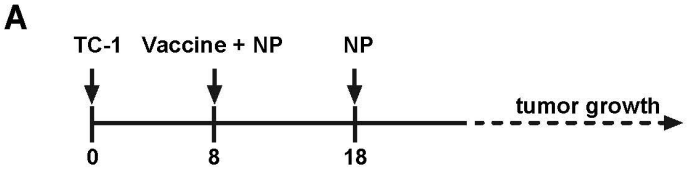

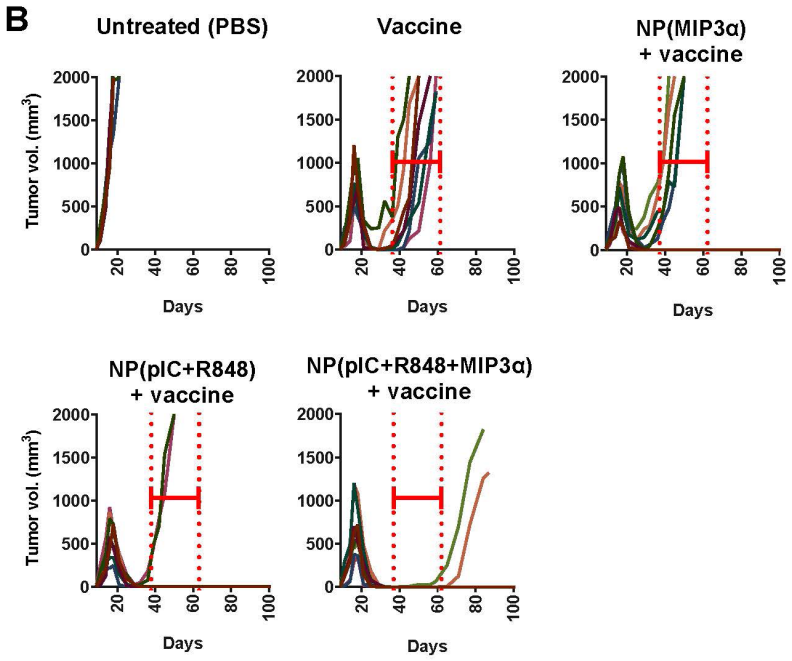

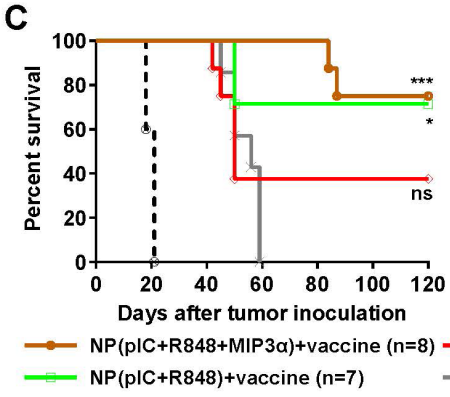

D

Comparison	P value
PBS vs. v	0.0007 ***
PBS vs. NP(MIP3α)+v	0.0003 ***
PBS vs. NP(pIC+R848)+v	0.0007 ***
PBS vs. NP(pIC+R848+MIP3α)+v	0.0003 ***
V vs. NP(MIP3α)+v	**0.5167 ns**
V vs. NP(pIC+R848)+v	**0.0195** *
V vs. NP(pIC+R848+MIP3α)+v	**0.0001** ***
NP(pIC+R848)+v vs. NP(MIP3α)+v	0.1499 ns
NP(pIC+R848)+v vs. NP(pIC+R848+MIP3α)+v	0.7845 ns
NP(pIC+R848+MIP3α)+v vs. NP(MIP3α)+v	0.0786 ns

Figure 4. Effective therapeutic efficacy improvement, upon NP co-treatment, persists in distinct therapeutic cancer vaccines >

The efficacy of the monotherapy of NP(pIC+R848+MIP3α) as well as combined with two distinct therapeutic cancer vaccines was determined. The RMA tumor bearing mice were vaccinated intradermally in the tail base at day 10 post tumor inoculation with a therapeutic synthetic long peptide vaccine containing both CD4 and CD8 epitopes against two viral proteins that is expressed by RMA cells. At the same time, the tumors were treated with an intratumoral injection with NPs at day 10 and at day 20. The TC-1 tumor bearing mice were vaccinated subcutaneously in the contralateral flank at day 8 post tumor inoculation with a therapeutic synthetic long peptide vaccine containing both CD4 and CD8 epitopes against the HPV E7 protein that is expressed by TC-1 cells. At the same time, the tumors were treated with an intratumoral injection with NPs at day 8 and at day 18. A) Tumor-growth data from day 0 to day 60 or day 80 for the PBS (control) group and three treatment groups (vaccine only, NP(pIC+R848+MIP3α) only, and vaccine plus NP(pIC+R848+MIP3α) combined) in the RMA (top) and TC-1 (bottom) models. B) Kaplan-Meier survival plots depicting progression-free survival and percent overall survival for the RMA model. C) Kaplan-Meier survival plots depicting progression-free survival and percent overall survival for the TC-1 model. Survival curves were compared using the log-rank test. Statistical differences were considered significant at * $p = < 0.05$; ** $p = < 0.01$; *** $p < 0.001$. Abbreviations: ns: not (statistically) significant; V: Vaccine.

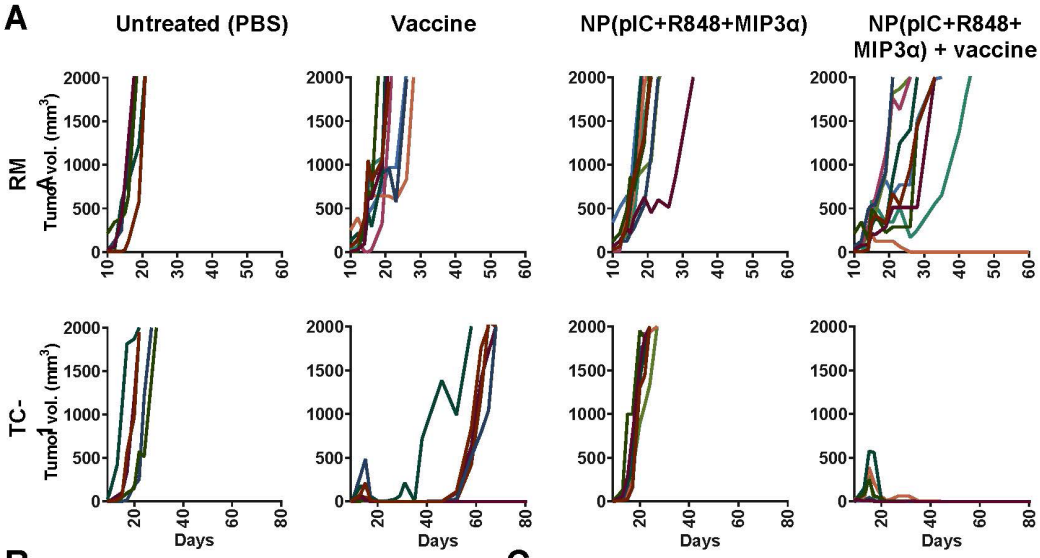

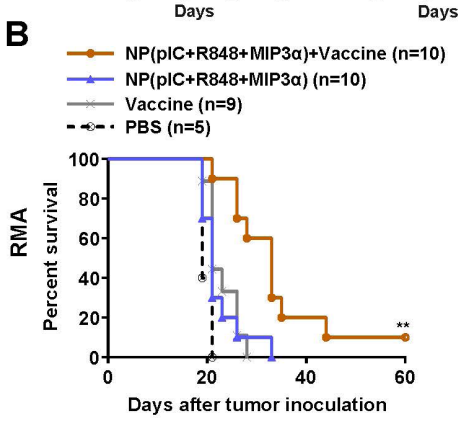

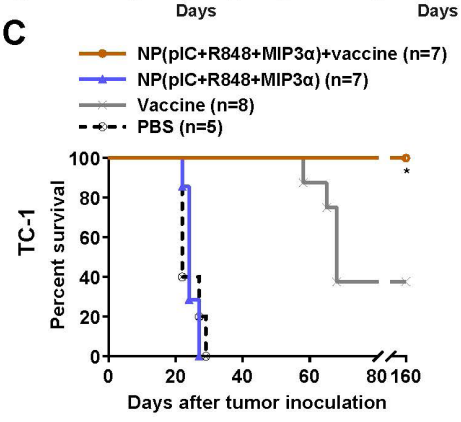

Comparison	P value
PBS vs. v	0.0259 *
PBS vs. NP(pIC+R848+MIP3α)	0.1354 ns
PBS vs. NP(pIC+R848+MIP3α)+v	0.0002 ***
V vs. NP(pIC+R848+MIP3α)	0.7201 ns
V vs. NP(pIC+R848+MIP3α)+v	0.0012 **
NP(pIC+R848+MIP3α) vs. NP(pIC+R848+MIP3α)+v	0.0017 **

Comparison	P value
PBS vs. v	0.0001 ***
PBS vs. NP(pIC+R848+MIP3α)	0.8874 ns
PBS vs. NP(pIC+R848+MIP3α)+v	0.0003 ***
V vs. NP(pIC+R848+MIP3α)	<0.0001 ***
V vs. NP(pIC+R848+MIP3α)+v	**0.0147** *
NP(pIC+R848+MIP3α) vs. NP(pIC+R848+MIP3α)+v	0.0002 ***

3.4. Effective therapeutic efficacy improvement, upon NP co-treatment, persists in distinct therapeutic cancer vaccines

Next, we expanded our approach to another cancer model with a different etiology. Thus, we applied our NP formulation in combination with an another therapeutic cancer vaccine modality aimed to induce adaptive immune responses against epitopes of the aggressive RMA T lymphoma model. The RMA bearing mice were treated with a therapeutic cancer vaccine administered intradermally in the tail base, at day 10, and consisted of a mixture of synthetic long peptides containing both CD4 and CD8 epitopes against two viral proteins that is expressed by RMA cells. The TC-1 bearing mice were vaccinated as per described previously. In addition, we also determined the efficacy of NP(pIC+R848+MIP3**α**) as a monotherapy (i.e. without vaccine co-treatment), in both TC-1 and the RMA models. To this end, TC-1 and RMA tumor bearing mice were treated twice with intratumoral injections and we observed that NP(pIC+R848+MIP3**α**), as a monotherapy, did not improve the survival of mice in neither TC-1 or RMA model (Figure 4A). However, the combination of the therapeutic cancer vaccine and the intratumoral administration of NP(pIC+R848+MIP3**α**) in both TC-1 and RMA successfully enhanced the mice survival significantly (Figure 4B and 4C). These results indicate that the intratumoral administration of NP(pIC+R848+MIP3**α**) improved the efficacy of two distinct therapeutic cancer vaccines in two aggressive cancer models.

3.5. Local NP treatment immune modulates the tumor microenvironment and the tumor-draining lymph node

Next, we determined the cell population alterations in the tumor and in the tumor-draining lymph node. For this purpose, we analyzed the lymphoid and myeloid populations within these organs of mice bearing TC-1 tumors. Mice were treated as described previously and the organs were resected and analyzed ex vivo at day 18. Cancer antigen-specific CD8+ T cells were detectable in the analyzed organs of vaccinated mice and the levels were not found to increase upon combined treatment (Figure S5A-B). As a monotherapy, NP(pIC+R848+MIP3**α**) increased the levels of CD8+ T cells and reduced the levels of CD4+, CD4+CD25+ Tregs and of CD49b+ NK cells in the tumor, but this difference was not statistically significant (Figure 5A). In the tumors of mice that were vaccinated or vaccinated and treated with NP(pIC+R848+MIP3**α**) the levels of CD45+, CD3+ and of CD8+ cells significantly increased and the levels of CD4+, CD4+CD25+ and of CD49b+ significantly

decreased (Figure 5A). In the tumor-draining lymph node, NP(pIC+R848+MIP3α) monotherapy as well as the combined treatment increased the levels of CD3+, CD4+ and of CD8+ cells, but this difference was not statistically significant (Figure 5B). On the other hand, the levels of CD49b+ decreased significantly.

Within the myeloid populations in the tumor, the combined treatment significantly increased the levels of CD11b+F4/80+ macrophages, reduced the levels of CD11b+F4/80+/Ly6G-Ly6Cmed tumor associated macrophages and increased the levels of CD11b+F4/80+/Ly6G-Ly6Chi inflammatory monocytes, but these differences were not statistically significant (Figure 5C). In the tumor-draining lymph node, NP(pIC+R848+MIP3α) monotherapy increased the levels of CD11b+Ly6G+ neutrophils significantly, and increased the levels CD11b+F4/80+/Ly6G-Ly6Chi inflammatory monocytes and decreased the levels of CD11b+F4/80+/Ly6G-Ly6Cmed tumor associated macrophages, but these differences were not statistically significant (Figure 5D). Similarly, the combination of vaccination and NP(pIC+R848+MIP3α) treatment increased the levels of CD11b+Ly6G-/Ly6Chi immature myeloid cells, CD11b+Ly6G+ neutrophils and of CD11b+F4/80+/Ly6G-Ly6Chi inflammatory monocytes significantly, and decreased the levels of CD11b+F4/80+/Ly6G-Ly6Cmed tumor-associated macrophages significantly in the tumor-draining lymph node (Figure 5D & S6). Moreover, the combination treatment of the vaccine and NP(pIC+R848+MIP3α) reduced the ratio of Ly6G-Ly6Cmed tumor-associated macrophages to Ly6G-Ly6Chi inflammatory monocytes significantly (Figure 5E).

These results combined indicate that the intratumoral administration of NP(pIC+R848+MIP3α) impacted both lymphoid and myeloid populations in the tumor and in the tumor-draining lymph. The most evident adjuvant effects of NP(pIC+R848+MIP3α) when combined with vaccination were a significant influx of macrophages into the tumor and a shift from suppressor tumor-associated macrophages towards an acute inflammatory phenotype in the tumor-draining lymph node. Overall, this indicates that the adaptive immune responses (lymphocytes) are potentiated while the innate immune responses acquire an activated state.

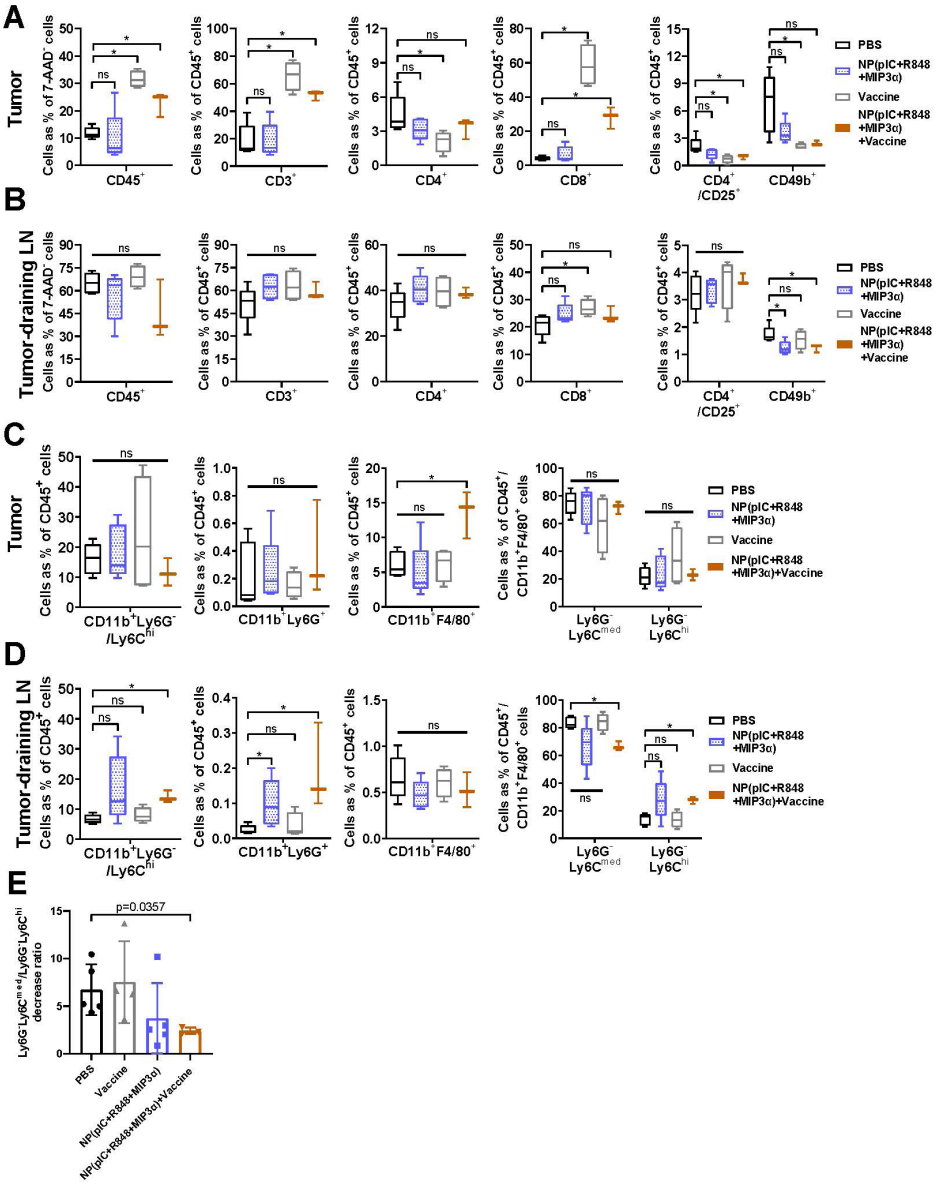
A
Tumor
Cells as % of 7-AAD- cells
CD45+
CD3+
CD4+
CD8+
CD4+ /CD25+
CD49b+
B
Tumor-draining LN
Cells as % of CD45+ cells
C
CD11b+Ly6G- /Ly6Chi
CD11b+Ly6G+
CD11b+F4/80+
Cells as % of CD45+/ CD11b+F4/80+ cells
Ly6G- Ly6Cmed
Ly6G- Ly6Chi
D
E
Ly6G-Ly6Cmed/Ly6G-Ly6Chi decrease ratio
p=0.0357
PBS
Vaccine
NP(pIC+R848+MIP3α)
NP(pIC+R848+MIP3α)+Vaccine
ns

< **Figure 5. Local NP treatment immune modulates the tumor microenvironment and the tumor-draining lymph node**

At day 8, four groups of mice (n=5 on average) with TC-1 tumors were treated as follows: 1) received an intratumoral injection of PBS (control); 2) received an intratumoral injection of NP(pIC+R848+MIP3α); 3) were vaccinated; or 4) were vaccinated and treated with an intratumoral injection of NP(pIC+R848+MIP3α). Ten days later, the intratumoral injections were repeated. At day 18, the tumors were resected and analyzed by flow cytometry: A) Lymphoid population analyzed within the tumor: CD45+ vaccine vs. PBS, p=0.0159; CD45+ vaccine plus NP(pIC+R848+MIP3α) vs. PBS, p=0.0357; CD3+ vaccine vs. PBS, p=0.0159; CD3+ vaccine plus NP(pIC+R848+MIP3α) vs. PBS, p=0.0357; CD4+ vaccine vs. PBS, p=0.0159; CD8+ vaccine vs. PBS, p=0.0159; CD8+ vaccine plus NP(pIC+R848+MIP3α) vs. PBS, p=0.0357; CD4+CD25+ vaccine vs. PBS, p=0.159; CD4+CD25+ vaccine plus NP(pIC+R848+MIP3α), p=0.0357; CD49b+ vaccine vs. PBS, p=0.0238. B) Lymphoid population analyzed within the tumor-draining lymph node: CD8+ vaccine vs. PBS, p=0.0317; CD49b+ NP(pIC+R848+MIP3α) vs. PBS, p=0.0397; CD49b+ vaccine plus NP(pIC+R848+MIP3α) vs. PBS, p=0.0357. C) Myeloid population analyzed within the tumor: CD11b+F4/80+ vaccine plus NP(pIC+R848+MIP3α) vs. PBS, p=0.0357. D) Myeloid population analyzed within the tumor-draining lymph node: CD11b+Ly6G-/Ly6Chi vaccine plus NP(pIC+R848+MIP3α) vs. PBS, p=0.0357; CD11b+Ly6G+ NP(pIC+R848+MIP3α) vs. PBS, p=0.0159; CD11b+Ly6G+ vaccine plus NP(pIC+R848+MIP3α) vs. PBS, p=0.0357; CD11b+F4/80+/Ly6G-Ly6Cmed vaccine plus NP(pIC+R848+MIP3α) vs. PBS, p=0.0357; CD11b+F4/80+/Ly6G-Ly6Chi vaccine plus NP(pIC+R848+MIP3α) vs. PBS, p=0.0357. E) Ly6G-Ly6Cmed/Ly6G-Ly6Chi (in the CD11b+F4/80+ gate) calculated decrease ratio in the tumor-draining lymph node upon described treatments: PBS vs. vaccine, p=0.9048; PBS vs. NP(pIC+R848+MIP3α), p=0.0952; PBS vs. vaccine plus NP(pIC+R848+MIP3α), p=0.0357. Statistics were calculated using a two-tailed Mann Whitney test. Statistical differences were considered significant at $p < 0.05$. * = $p < 0.05$; ** $p = < 0.01$; *** $p < 0.001$. Tregs defined as CD4+CD25+ within the 7-AAD-/CD45+ gate; NK cells defined as CD49b+ within the 7-AAD-/CD45+ gate; Immature myeloid cell population, defined as CD11b+Ly6G-/Ly6C+ cells within the 7-AAD-/CD45+ gate; Neutrophils defined as CD11b+Ly6G+ cells within the 7-AAD-/CD45+ gate; Macrophages defined as CD11b+F4/80+ cells within the 7-AAD-/CD45+ gate; Tumor-associated macrophages defined as Ly6G-Ly6Cmed cells within the CD11b+F4/80+ and the 7-AAD-/CD45+ gate; Inflammatory monocytes defined as Ly6G-Ly6Chi cells within the CD11b+F4/80+ and the 7-AAD-/CD45+ gate. Abbreviations: ns: not (statistically) significant.

4. DISCUSSION

We have rationally developed a practical strategy to improve cancer vaccines by the NP mediated delivery of two TLR agonists and a chemokine to the tumor and tumor-draining lymph node. It takes advantage of the robust induction of cancer fighting T cells by the cancer vaccines while ameliorating the local negative immune regulation. Mechanistically, the combined treatment induced high influx of macrophages into the tumor and induced a shift from suppressor tumor-associated macrophages towards an acute inflammatory phenotype in the tumor-draining lymph node.

Based on our findings, we hypothesize that only a portion of the injected NPs into TC-1 tumors are actually endocytosed by cancer cells, T-regs, MDSC, macrophages and other cells. The NPs that are not endocytosed continue the slow release pIC, R848 and MIP3α into the tumor area or drain to the tumor-draining lymph node where they continue to amplify acute innate and adaptive immune responses (Figure 6).

Figure 6. Rational design to improve the efficacy of therapeutic cancer vaccines by the co-delivery of immune adjuvants to the tumor and tumor-draining lymph node >

Step 1) The NPs are injected in the tumors, whereby pIC and R848 skew the tumor microenvironment and tumor-draining lymph node from a suppressive and chronic inflamed towards an acute inflamed milieu. A portion of the injected NPs are partially endocytosed by cancer cells, T-regs, MDSC, macrophages and other cells, activating immune responses. The NPs that were not endocytosed continue the slow release of pIC, R848 and MIP3α into the tumor area further maintaining an immune activated state. **Step 2)** Another portion of the NPs that were not endocytosed by cells in the tumor, as well as some of the previously released pIC, R848 and MIP3α, partially drain to the tumor-draining lymph node. The pIC and R848 activate residing immature and suppressed immune cells and MIP3α attracts immune cells. **Step 3)** Unaffected by the local negative regulation and robustly activated T cells against cancer antigens are induced by the therapeutic cancer vaccine. **Step 4)** Adaptive and innate immune cells proliferate and are stimulated in the spleen and lymph nodes. **Step 5)** The remaining MIP3α in the tumor and tumor-draining lymph node actively recruits more cancer fighting immune cells to the tumor bed and mediate tumor mass regression. This figure was composed using Servier Medical Art templates, which are licensed under a Creative Commons Attribution 3.0 Unported License; https://smart.servier.com.

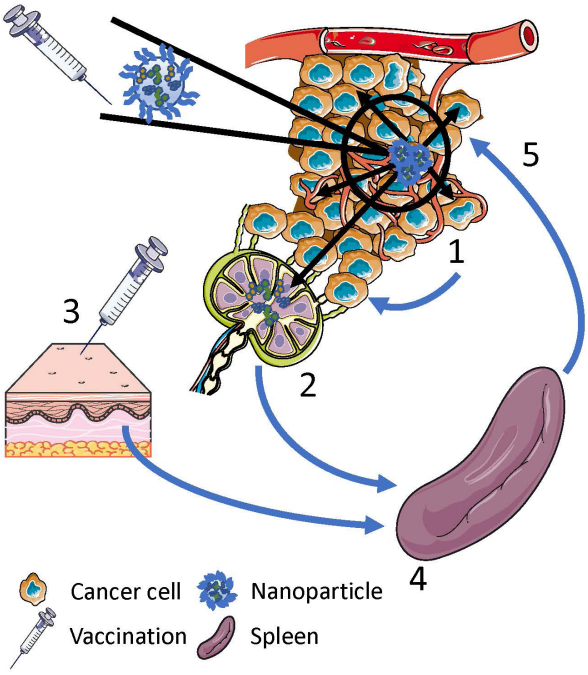

1. Local injection of immune modulators in nanoparticles induces local acute inflammation

2. Partial drainage of immune modulators to the tumor-draining lymph node

3. Induction of cytotoxic T cells against cancer epitopes by therapeutic cancer vaccine

4. Systemic activation of adaptive and innate immune responses

5. Active recruitment of immune cells to the tumor.

After screening the potential of pIC, R848 and MIP3α in NPs as a monotherapy, we identified the combination to be the most potent form in the TC-1 cancer model and later in the RMA cancer model. Interestingly, a possible intrinsic therapeutic effect was observed by the vehicle control NP(empty) and vaccination. While the PLGA NPs themselves are non-cytotoxic and biocompatible, the direct activation of the inflammasome by PLGA and subsequent secretion of interleukin-1β by DCs has been reported which may explain the observed effect [38,39].

In the TC-1 cancer model, we show that well established and large tumors up to 1200 mm3 were successfully eradicated with the combined treatment and that the mice survival was improved from 0-40 percent to 75-100 percent. Furthermore, we show that the intratumoral administration of NP(pIC+R848+MIP3α) profoundly impacted lymphoid and myeloid populations in the tumor and tumor-draining lymph node. Moreover, intratumoral administration of NP(pIC+R848+MIP3α) after vaccination induced considerable increases in circulating cancer antigen-specific CD8+ T cells, compared to vaccinated only mice, leading to more tumor eradications. Despite that the survival results in the RMA model are relatively less impressive compared to the TC-1 model, the gain in progression-free survival after combined treatment is yet remarkable considering the much higher proliferation rate of the RMA cells compared to TC-1 cells, as 1x105 TC-1 cells are injected into mice compared to only 1x103 RMA cells to achieve similar tumor sizes at day 8-10. We prepared PEGylated PLGA NPs with an average size ranging from 140 to 270 nm, which is within the optimal functional range (40 nm to 300 nm) reported for durable half-life and sustained drug release [40–42]. We injected the NPs intratumoral to reduce, but not eliminate, systemic distribution and maintain high local confinement of these immune adjuvants to the tumor area despite that intravenous injection would also concentrate NPs in the tumor, but likely less efficiently whilst possibly inducing more side-effects.

The chemokine MIP3α by itself did not significantly improve the cancer vaccine efficacy but when combined with pIC and R848 the progression-free survival was nearly doubled. In addition to the observed influx of macrophages to the tumor, this could be an indication of a functional effect other than the induction of chemotaxis. MIP3α is commonly produced by several tumor types and is often described as ambivalent, having both anti and pro cancer effects, exhibiting pleiotropic immune responses [43]. Despite its controversial role, it is not surprising that arriving immune

cells, attracted by MIP3α to the highly suppressed tumor microenvironment, may become also suppressive and dysfunctional. However, if the arriving immune cells encounter a less immune suppressed microenvironment, as artificially induced by TLR agonists for example (as proposed here), it is conceivable that then MIP3α plays an anti-cancer role. Indeed, a similar observation was made by Fushimi et al. that demonstrated that the intratumoral injection of adenovirus-mediated gene transfer of MIP3α suppressed tumor growth, but only on cancer models that are highly immunogenic, and this process was mediated by DCs and lymphocytes [44]. Furthermore, we sought to broaden our understanding on possible mechanisms by which the efficacy of the combined treatment is enhanced by focusing on several types of immune cells and the differences in lymphoid and myeloid cell populations upon treatment compared to mock treated tumors. Upon monotherapy with NP(pIC+R848+MIP3α) (i.e. without vaccine), more CD8 T cells and less CD4+CD25+ regulatory T cells and CD49b+ NK cells were found in the tumor area which is consistent with previous observations [45]. The myeloid population in the tumor microenvironment appeared to be less prone to immune modulation with monotherapy of NP(pIC+R848+MIP3α) in TC-1 tumors. This could be due to tumor cells overcoming acute inflammatory cytokines triggered by the TLR agonists, or the NPs and/or most of the TLR agonists do not remain in the tumor and drain to the tumor-draining lymph node. However, the monotherapy with NP(pIC+R848+MIP3α) did affect the myeloid population in the tumor-draining lymph node as more neutrophils were observed and within the macrophage population a shift in phenotype from suppressor tumor-associated macrophages towards inflammatory monocyte phenotype was observed. Furthermore, it is possible that this observed effect was due to the direct effect of TLR agonists drained from the tumor or due to a secondary effect caused by other signals draining from the tumor area. Nonetheless, our results are in line with the finds of Muraoka et al. that described that tumor immune resistance is highly mediated by suppressor tumor-associated macrophages and the activation of these cells rendered tumors sensitive to adaptive immune responses [46].

The changes observed upon combined treatment of vaccination with NP(pIC+R848+MIP3α) that were not observed in the vaccinated only mice resembled the effects observed upon NP(pIC+R848+MIP3α) monotherapy with the addition of an almost three-fold increase of macrophages in the tumor. This may be an indication that besides T cells, enough numbers of properly activated macrophages are necessary to avoid tumor recurrences as observed by the significantly higher percentages of complete remissions and very late relapses compared to vaccinated only mice.

Most pre-clinical studies to date have focused on the delivery of TLR agonists together with antigens to boost vaccines potency by enhancing DC priming and maturation [13]. Either the antigens and TLR agonists are in soluble form, separate or conjugated, or even in a nanovesicle, but most commonly not intended to be delivered directly to the tumor [47]. In our own experiments, we administered the cancer vaccines combined with the TLR9 agonist CpG, either intradermally or subcutaneously, but in an anatomical location separate to the tumor, to induce robust antigen specific T cells. However, the mere vaccination with antigen and CpG did not result in high percentages of durable tumor clearances. On the other hand, the systemic administration and adjuvant effect of pIC combined with peptide vaccination was studied by Mohamed et al. [48]. Although our data is in line with the authors observations, such as an increase of antigen-specific CD8 T cells, the mice where not challenged with a tumor and therefore it is unclear whether systemic administration of pIC could possibly lead to more tumor clearances. Intratumoral mono immunotherapy with PRR agonists, including TLR agonists, are reported successful modalities to reduce the immunosuppressive activity in the tumor microenvironment, revert resistance to immune checkpoint inhibitors (including PD-1) and enhancing tumor eradications in several mice tumor models [49,50].

Although therapeutic cancer vaccines succeed in inducing robust cancer fighting T cells leading to temporary tumor shrinkage, our data indicates that (local) immune modulation is necessary for durable tumor eradications likely due to the functional abrogation of immune suppressor cells (T-regs, MDSCs, TAMs), boosting T cells function (inhibit senescence) and actively implicate the innate immune system in a coordinated effort to fully clear all cancer cells (Figure 7).

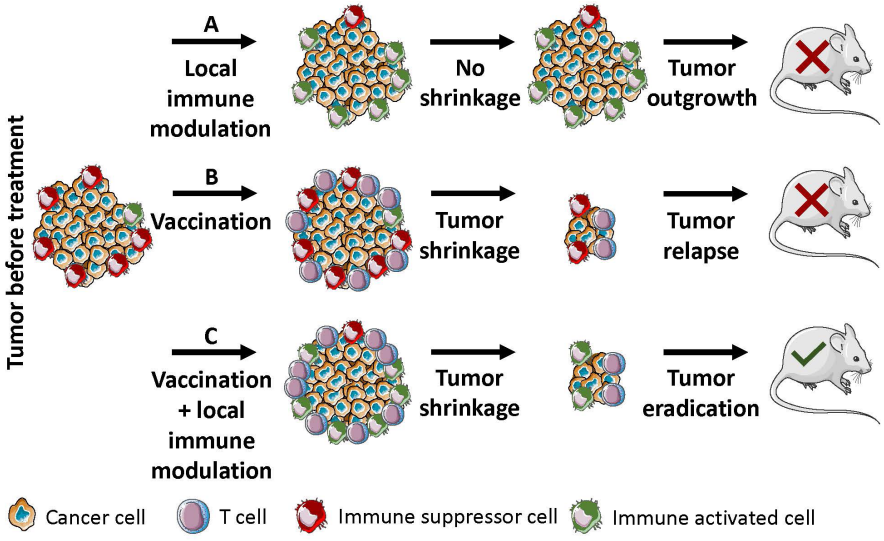

Figure 7. Hypothetical therapeutic cancer vaccine improved efficacy proposed putative mechanism

A) Local immune modulation induces immune phenotype shift from suppressor (red cells) to activated type (green cells) but this has little effect in tumors without T cells. **B)** Vaccination only induces the influx of T cells (purple cells) into the tumor. However, the strong immune suppressed environment (red cells) is not alleviated and full tumor clearance is not achieved leading to tumor relapses. **C**) Vaccination and local immune modulation therapy combined induces the influx of T cells (purple cells) into the tumor. Concurrently, the local immune modulation therapy induces a shift from suppressor (red cells) to activate (green cells) immune phenotype which together with the T cells achieves full tumor clearances. This figure was composed using Servier Medical Art templates, which are licensed under a Creative Commons Attribution 3.0 Unported License; https://smart.servier.com.

As we have shown, our results indicate that the NP mediated co-delivery of immune modulators alters the lymphoid and myeloid cell levels and phenotype contributing to the amelioration of negative regulation. Consequently, the efficacy of cancer vaccines to eradicate tumors is enhanced.

Grant Support
This work is part of the research programme 723.012.110 (Vidi), which is financed by the Netherlands Organisation for Scientific Research (NWO). Also, we would like to thank the financial support of the LUMC fellowship grant, project grants from the EU Program H2020-MSCA-2015-RISE (644373– PRISAR) and MSCA-ITN-2015-ETN (675742-ISPIC), H2020-MSCA-2016-RISE (734684-CHARMED) and H2020-MSCA-RISE-2017-CANCER (777682).

Declaration of interest
The authors were supported with funding from Leiden University Medical Center and the Netherlands Organization for Scientific Research (NWO). The authors have no other relevant affiliations or financial involvement with any organization or entity with a financial interest in, or financial conflict with, the subject matter or materials discussed in the manuscript, apart from those already disclosed.

Author contributions
L.J. Cruz and F. Ossendorp designed and supervised the study. C.G. Da Silva wrote the manuscript and performed the experiments. L.J. Cruz and C.G. Da Silva assembled the nanoparticles. M.G.M. Camps supported the animal studies. T.M.W.Y. Li performed the cell immunofluorescence, NP uptake assay and supported the preparation of the tumor samples for tumor microenvironment analysis. A.B. Chan revised the paper.

Data availability
The authors declare that all the data related with this study are available within the paper or can be obtained from the authors on request.

REFERENCES

[1] S.H. van der Burg, R. Arens, F. Ossendorp, T. van Hall, C.J.M. Melief, Vaccines for established cancer: overcoming the challenges posed by immune evasion, Nat. Rev. Cancer. 16 (2016) 219–233. doi:10.1038/nrc.2016.16.

[2] M.A. Cheever, C.S. Higano, PROVENGE (Sipuleucel-T) in Prostate Cancer: The First FDA-Approved Therapeutic Cancer Vaccine, Clin. Cancer Res. 17 (2011) 3520–3526. doi:10.1158/1078-0432.CCR-10-3126.

[3] H. Maeng, M. Terabe, J.A. Berzofsky, Cancer vaccines: translation from mice to human clinical trials, Curr. Opin. Immunol. 51 (2018) 111–122. doi:10.1016/J.COI.2018.03.001.

[4] R.M. Luiten, E.W.M. Kueter, W. Mooi, M.P.W. Gallee, E.M. Rankin, W.R. Gerritsen, S.M. Clift, W.J. Nooijen, P. Weder, W.F. van de Kasteele, J. Sein, P.C.M. van den Berk, O.E. Nieweg, A.M. Berns, H. Spits, G.C. de Gast, Immunogenicity, including vitiligo, and feasibility of vaccination with autologous GM-CSF-transduced tumor cells in metastatic melanoma patients., J. Clin. Oncol. 23 (2005) 8978–91. doi:10.1200/JCO.2005.01.6816.

[5] Z. Ye, Q. Qian, H. Jin, Q. Qian, Cancer vaccine: learning lessons from immune checkpoint inhibitors., J. Cancer. 9 (2018) 263–268. doi:10.7150/jca.20059.

[6] R.W. Jenkins, D.A. Barbie, K.T. Flaherty, Mechanisms of resistance to immune checkpoint inhibitors, Br. J. Cancer. 118 (2018) 9–16. doi:10.1038/bjc.2017.434.

[7] S. Kouidhi, A.B. Elgaaied, S. Chouaib, Impact of Metabolism in on T-Cell Differentiation and Function and Cross Talk with Tumor Microenvironment, Front. Immunol. 8 (2017) 270. doi:10.3389/fimmu.2017.00270.

[8] J. Ye, X. Huang, E.C. Hsueh, Q. Zhang, C. Ma, Y. Zhang, M.A. Varvares, D.F. Hoft, G. Peng, Human regulatory T cells induce T-lymphocyte senescence, Blood. 120 (2012) 2021–2031. doi:10.1182/blood-2012-03-416040.

[9] C. Devaud, L.B. John, J.A. Westwood, P.K. Darcy, M.H. Kershaw, Immune modulation of the tumor microenvironment for enhancing cancer immunotherapy., Oncoimmunology. 2 (2013) e25961. doi:10.4161/onci.25961.

[10] A. Marabelle, H. Kohrt, C. Caux, R. Levy, Intratumoral immunization: a new paradigm for cancer therapy., Clin. Cancer Res. 20 (2014) 1747–56. doi:10.1158/1078-0432.CCR-13-2116.

[11] C. Pasare, R. Medzhitov, Toll-Like Receptors: Linking Innate and Adaptive Immunity, in: Mech. Lymph. Act. Immune Regul. X, Springer US, Boston, MA, 2005: pp. 11–18. doi:10.1007/0-387-24180-9_2.

[12] M. Shi, X. Chen, K. Ye, Y. Yao, Y. Li, Application potential of toll-like receptors in cancer immunotherapy: Systematic review., Medicine (Baltimore). 95 (2016) e3951. doi:10.1097/MD.0000000000003951.

[13] B. Temizoz, E. Kuroda, K.J. Ishii, Vaccine adjuvants as potential cancer immunotherapeutics, Int. Immunol. 28 (2016) 329–338. doi:10.1093/intimm/dxw015.

[14] J.K. Dowling, A. Mansell, Toll-like receptors: the swiss army knife of immunity and vaccine development., Clin. Transl. Immunol. 5 (2016) e85. doi:10.1038/cti.2016.22.

[15] Y. Yang, C.-T. Huang, X. Huang, D.M. Pardoll, Persistent Toll-like receptor signals are required for reversal of regulatory T cell–mediated CD8 tolerance, Nat. Immunol. 5 (2004) 508–515. doi:10.1038/ni1059.

[16] L. Huang, H. Xu, G. Peng, TLR-mediated metabolic reprogramming in the tumor microenvironment: potential novel strategies for cancer immunotherapy, Cell. Mol. Immunol. (2018). doi:10.1038/cmi.2018.4.

[17] H. Chi, C. Li, F.S. Zhao, L. Zhang, T.B. Ng, G. Jin, O. Sha, Anti-tumor Activity of Toll-Like Receptor 7 Agonists., Front. Pharmacol. 8 (2017) 304. doi:10.3389/fphar.2017.00304.

[18] M.C. Dieu, B. Vanbervliet, A. Vicari, J.M. Bridon, E. Oldham, S. Aït-Yahia, F. Brière, A. Zlotnik, S. Lebecque, C. Caux, Selective recruitment of immature and mature dendritic cells by distinct chemokines expressed in different anatomic sites., J. Exp. Med. 188 (1998) 373–86. doi:10.1084/JEM.188.2.373.

[19] A. Al-Aoukaty, B. Rolstad, A. Giaid, A.A. Maghazachi, MIP-3alpha, MIP-3beta and fractalkine induce the locomotion and the mobilization of intracellular calcium, and activate the heterotrimeric G proteins in human natural killer cells, Immunology. 95 (1998) 618–624. doi:10.1046/j.1365-2567.1998.00603.x.

[20] F. Liao, R.L. Rabin, C.S. Smith, G. Sharma, T.B. Nutman, J.M. Farber, CC-chemokine receptor 6 is expressed on diverse memory subsets of T cells and determines responsiveness to macrophage inflammatory protein 3 alpha., J. Immunol. 162 (1999) 186–94.

[21] E.V. Acosta-Rodriguez, L. Rivino, J. Geginat, D. Jarrossay, M. Gattorno, A. Lanzavecchia, F. Sallusto, G. Napolitani, Surface phenotype and antigenic specificity of human interleukin 17–producing T helper memory cells, Nat. Immunol. 8 (2007) 639–646. doi:10.1038/ni1467.

[22] S. Yamashiro, J.M. Wang, D. Yang, W.H. Gong, H. Kamohara, T. Yoshimura, Expression of CCR6 and CD83 by cytokine-activated human neutrophils., Blood. 96 (2000) 3958–63.

[23] E. Schutyser, S. Struyf, J. Van Damme, The CC chemokine CCL20 and its receptor CCR6, Cytokine Growth Factor Rev. 14 (2003) 409–426. doi:10.1016/S1359-6101(03)00049-2.

[24] B. Kwong, H. Liu, D.J. Irvine, Induction of potent anti-tumor responses while eliminating systemic side effects via liposome-anchored combinatorial immunotherapy, (2011). doi:10.1016/j.biomaterials.2011.03.067.

[25] C.G. Da Silva, G.J. Peters, F. Ossendorp, L.J. Cruz, The potential of multi-compound nanoparticles to bypass drug resistance in cancer, Cancer Chemother. Pharmacol. 80 (2017) 881–894. doi:10.1007/s00280-017-3427-1.

[26] H.K. Makadia, S.J. Siegel, Poly Lactic-co-Glycolic Acid (PLGA) as Biodegradable Controlled Drug Delivery Carrier., Polymers (Basel). 3 (2011) 1377–1397. doi:10.3390/polym3031377.

[27] D.A. LaVan, T. McGuire, R. Langer, Small-scale systems for in vivo drug delivery, Nat. Biotechnol. 21 (2003) 1184–1191. doi:10.1038/nbt876.

[28] L.J. Cruz, P.J. Tacken, C. Eich, F. Rueda, R. Torensma, C.G. Figdor, Controlled release of antigen and Toll-like receptor ligands from PLGA nanoparticles enhances immunogenicity, Nanomedicine. 12 (2017) 491–510. doi:10.2217/nnm-2016-0295.

[29] L.J. Cruz, P.J. Tacken, F. Rueda, J.C. Domingo, F. Albericio, C.G. Figdor, Targeting Nanoparticles to Dendritic Cells for Immunotherapy, in: Methods Enzymol., 2012: pp. 143–163. doi:10.1016/B978-0-12-391858-1.00008-3.

[30] L.J. Cruz, P.J. Tacken, F. Bonetto, S.I. Buschow, H.J. Croes, M. Wijers, I.J. de Vries, C.G. Figdor, Multimodal Imaging of Nanovaccine Carriers Targeted to Human Dendritic Cells, Mol. Pharm. 8 (2011) 520–531. doi:10.1021/mp100356k.

[31] L.J. Cruz, P.J. Tacken, R. Fokkink, B. Joosten, M.C. Stuart, F. Albericio, R. Torensma, C.G. Figdor, Targeted PLGA nano- but not microparticles specifically deliver antigen to human dendritic cells via DC-SIGN in vitro, J. Control. Release. 144 (2010) 118–126. doi:10.1016/j.jconrel.2010.02.013.

[32] J. Tel, A.J.A. Lambeck, L.J. Cruz, P.J. Tacken, I.J.M. de Vries, C.G. Figdor, Human Plasmacytoid Dendritic Cells Phagocytose, Process, and Present Exogenous Particulate Antigen, J. Immunol. 184 (2010) 4276–4283. doi:10.4049/jimmunol.0903286.

[33] K.Y. Lin, F.G. Guarnieri, K.F. Staveley-O'Carroll, H.I. Levitsky, J.T. August, D.M. Pardoll, T.C. Wu, Treatment of established tumors with a novel vaccine that enhances major histocompatibility class II presentation of tumor antigen., Cancer Res. 56 (1996) 21–6.

[34] H.G. Ljunggren, K. Kärre, Host resistance directed selectively against H-2-deficient lymphoma variants. Analysis of the mechanism, J. Exp. Med. 162 (1985) 1745–1759. doi:10.1084/jem.162.6.1745.

[35] F. Ossendorp, N. Fu, M. Camps, F. Granucci, S.J.P. Gobin, P.J. van den Elsen, D. Schuurhuis, G.J. Adema, G.B. Lipford, T. Chiba, A. Sijts, P.-M. Kloetzel, P. Ricciardi-Castagnoli, C.J.M. Melief, Differential Expression Regulation of the and Subunits of the PA28 Proteasome Activator in Mature Dendritic Cells, J. Immunol. 174 (2005) 7815–7822 doi:10.4049/jimmunol.174.12.7815.

[36] G.G. Zom, S. Khan, C.M. Britten, V. Sommandas, M.G.M. Camps, N.M. Loof, C.F. Budden, N.J. Meeuwenoord, D. V. Filippov, G.A. van der Marel, H.S. Overkleeft, C.J.M. Melief, F. Ossendorp, Efficient Induction of Antitumor Immunity by Synthetic Toll-like Receptor Ligand-Peptide Conjugates, Cancer Immunol. Res. 2 (2014) 756–764. doi:10.1158/2326-6066.CIR-13-0223.

[37] S. Zwaveling, S.C. Ferreira Mota, J. Nouta, M. Johnson, G.B. Lipford, R. Offringa, S.H. van der Burg, C.J.M. Melief, Established human papillomavirus type 16-expressing tumors are effectively eradicated following vaccination with long peptides., J. Immunol. 169 (2002) 350–8.

[38] F.A. Sharp, D. Ruane, B. Claass, E. Creagh, J. Harris, P. Malyala, M. Singh, D.T. O'Hagan, V. Pétrilli, J. Tschopp, L.A.J. O'Neill, E.C. Lavelle, Uptake of particulate vaccine adjuvants by dendritic cells activates the NALP3 inflammasome., Proc. Natl. Acad. Sci. U. S. A. 106 (2009) 870–5. doi:10.1073/pnas.0804897106.

[39] J. Wolfram, M. Zhu, Y. Yang, J. Shen, E. Gentile, D. Paolino, M. Fresta, G. Nie, C. Chen, H. Shen, M. Ferrari, Y. Zhao, Safety of Nanoparticles in Medicine., Curr. Drug Targets. 16 (2015) 1671–81. doi:10.2174/1389450115666140804124808

[40] R.C. Mundargi, V.R. Babu, V. Rangaswamy, P. Patel, T.M. Aminabhavi, Nano/micro technologies for delivering macromolecular therapeutics using poly(d,l-lactide-co-glycolide) and its derivatives, J. Control. Release. 125 (2008) 193–209. doi:10.1016/J.JCONREL.2007.09.013.

[41] S.M. Moghimi, A.C. Hunter, T.L. Andresen, Factors Controlling Nanoparticle Pharmacokinetics: An Integrated Analysis and Perspective, Annu. Rev. Pharmacol. Toxicol. 52 (2012) 481–503. doi:10.1146/annurev-pharmtox-010611-134623.

[42] S. Bhattacharjee, DLS and zeta potential – What they are and what they are not?, J. Control. Release. 235 (2016) 337–351. doi:10.1016/j.jconrel.2016.06.017.

[43] R. Ranasinghe, R. Eri, Modulation of the CCR6-CCL20 Axis: A Potential Therapeutic Target in Inflammation and Cancer, Medicina (B. Aires). 54 (2018). doi:10.3390/MEDICINA54050088.

[44] T. Fushimi, A. Kojima, M.A. Moore, R.G. Crystal, Macrophage inflammatory protein 3alpha transgene attracts dendritic cells to established murine tumors and suppresses tumor growth., J. Clin. Invest. 105 (2000) 1383–93. doi:10.1172/JCI7548.

[45] R.-F. Wang, Y. Miyahara, H.Y. Wang, Toll-like receptors and immune regulation: implications for cancer therapy, Oncogene. 27 (2008) 181–189. doi:10.1038/sj.onc.1210906.

[46] D. Muraoka, N. Seo, T. Hayashi, Y. Tahara, K. Fujii, I. Tawara, Y. Miyahara, K. Okamori, H. Yagita, S. Imoto, R. Yamaguchi, M. Komura, S. Miyano, M. Goto, S. Sawada, A. Asai, H. Ikeda, K. Akiyoshi, N. Harada, H. Shiku, Antigen delivery targeted to tumor-associated macrophages overcomes tumor immune resistance, J. Clin. Invest. 129 (2019) 1278–1294. doi:10.1172/JCI97642.

[47] G.G. Zom, S. Khan, C.M. Britten, V. Sommandas, M.G.M. Camps, N.M. Loof, C.F. Budden, N.J. Meeuwenoord, D. V. Filippov, G.A. van der Marel, H.S. Overkleeft, C.J.M. Melief, F. Ossendorp, Efficient Induction of Antitumor Immunity by Synthetic Toll-like Receptor Ligand-Peptide Conjugates, Cancer Immunol. Res. 2 (2014) 756–764. doi:10.1158/2326-6066.CIR-13-0223.

[48] M.L. Salem, S.A. EL-Naggar, A. Kadima, W.E. Gillanders, D.J. Cole, The adjuvant effects of the toll-like receptor 3 ligand polyinosinic-cytidylic acid poly (I:C) on antigen-specific CD8+ T cell responses are partially dependent on NK cells with the induction of a beneficial cytokine milieu, Vaccine. 24 (2006) 5119–5132. doi:10.1016/J.VACCINE.2006.04.010.

[49] R. Zhang, M.M. Billingsley, M.J. Mitchell, Biomaterials for vaccine-based cancer immunotherapy, J. Control. Release. 292 (2018) 256–276. doi:10.1016/J.JCONREL.2018.10.008.

[50] S. Wang, J. Campos, M. Gallotta, M. Gong, C. Crain, E. Naik, R.L. Coffman, C. Guiducci, Intratumoral injection of a CpG oligonucleotide reverts resistance to PD-1 blockade by expanding multifunctional CD8+ T cells., Proc. Natl. Acad. Sci. U. S. A. 113 (2016) E7240–E7249. doi:10.1073/pnas.1608555113.

CO-DELIVERY OF IMMUNOMODULATORS IN BIODEGRADABLE NANOPARTICLES IMPROVES THERAPEUTIC EFFICACY OF CANCER VACCINES

Da Silva, C.G., Camps, M.G.M., Li, T.M.W.Y., Chan, A.B., Ossendorp, F., Cruz L.J.

Biomaterials. 2019 Nov; 220:119417.

Supplementary Figures

Figure S1.
RMA MHC class I H-2Kb/Db expression
Figure S2.
The size and zeta potential data characterized by dynamic light scattering
Figure S3.
Tumor re-challenge and development of functional immunological memory against cancer epitopes
Figure S4.
Co-delivery of NPs containing pIC enhances the levels of circulating cancer antigen-specific CD8+ T cells
Figure S5.
Cancer antigen-specific T cells in the tumor and the tumor-draining lymph node
Figure S6.
Macrophage population phenotype shift in the tumor-draining lymph node upon treatment with immunomodulators

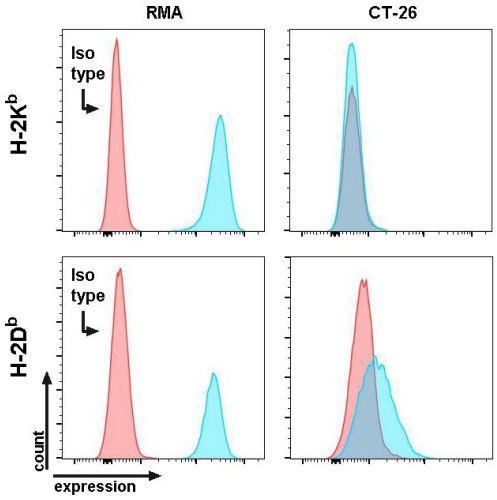

Figure S1. RMA MHC class I H-2Kb/Db expression

The expression of RMA MHC class I H-2Kb/Db was verified before in-vivo experiments to ascertain that the expression was not lost due to cell passages (expression in blue, red is isotype control). CT-26 was used as a negative control.

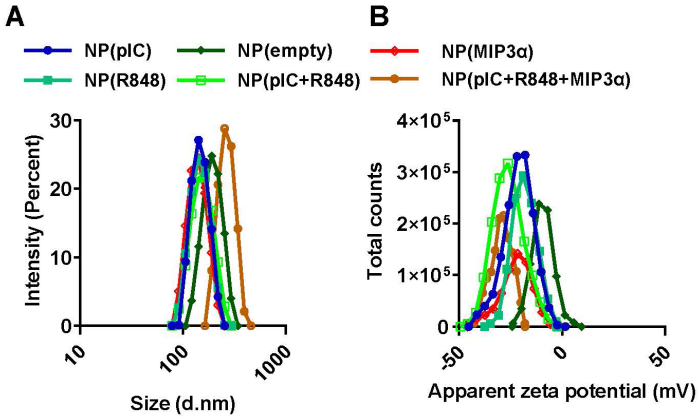

Figure S2. The size and zeta potential data characterized by dynamic light scattering

The size (A) and zeta potential (B) data distributions represent the mean value ± SD of 10 readings.

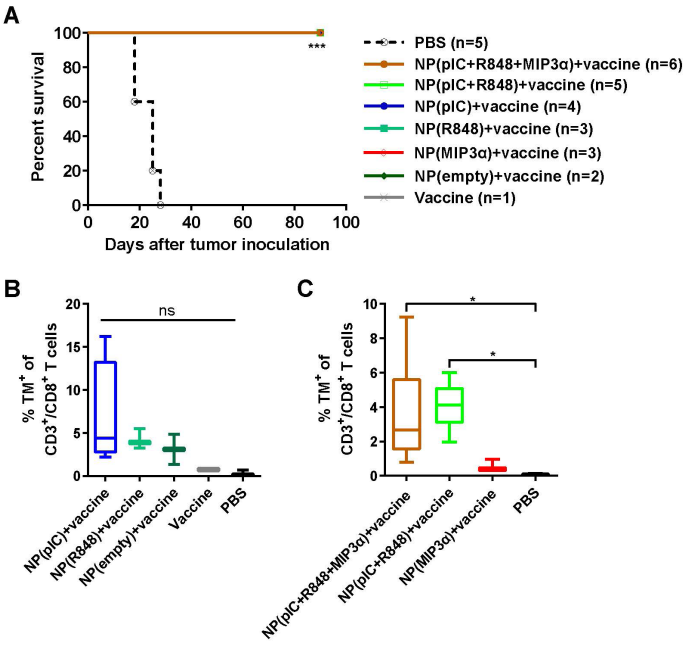

Figure S3. Tumor re-challenge and development of functional immunological memory against cancer epitopes

A) Kaplan-Meier survival plot depicting progression-free survival and percent overall survival of pooled data from two separate experiments for mice re-challenged with TC-1 cancer cells at day 120. Survival curves were compared using the log-rank test. B) The levels of TM+ T cells in blood of mice ten days after tumor re-challenge for mice treated with vaccination plus NP(pIC), vaccination plus NP(R848), vaccination plus NP(empty), vaccinated only and mock treated (PBS): NP(pIC)+vaccine vs. PBS p=0.0571; NP(R848)+vaccine vs. PBS p=0.100; NP(empty)+vaccine vs. PBS p=0.200. C) The levels of TM+ T cells in blood of mice ten days after tumor re-challenge for mice treated with vaccination plus NP(pIC+R848), vaccination plus NP(pIC+R848+MIP3α), vaccination plus NP(MIP3α) and mock treated (PBS): NP(pIC+R848+MIP3α)+vaccine vs. PBS p=0.0238; NP(pIC+R848)+vaccine vs. PBS p=0.0357; NP(MIP3α)+vaccine vs. PBS p=0.100. Statistics were calculated using a two-tailed Mann Whitney test. Statistical differences were considered significant at $p < 0.05$. * = $p < 0.05$; ** $p = < 0.01$; *** $p < 0.001$. Data plotted are presented as min to max. Abbreviations: ns: not (statistically) significant; TM: tetramer.

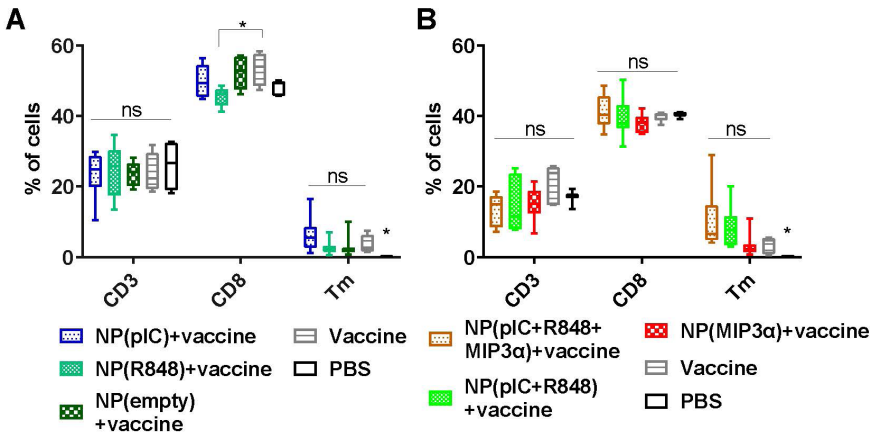

Figure S4. Co-delivery of NPs containing pIC enhances the levels of circulating cancer antigen-specific CD8+ T cells

Quantification of CD3+, CD8+ and the HPV16 E7 tetramer (TM) specific T cells in blood at day 16 (8 days post-treatment) after treatment with intratumoral NPs containing different immune adjuvants as compared with vaccine only or PBS (control). A) The levels of CD3+, CD8+ and TM+ T cells in control (PBS) mice and mice vaccinated as well as vaccinated and treated with NP(pIC), NP(R848) or NP(empty). B) The levels of CD3+, CD8+ and TM+ T cells in control (PBS) mice and mice vaccinated as well as vaccinated and treated with NP(MIP3α), NP(pIC+R848) or NP(pIC+R848+MIP3α). For TM levels: Vaccine vs. PBS p=0.0159 and p=0.0357, respectively. Statistics were calculated using a two-tailed Mann Whitney test. Statistical differences were considered significant at * p = < 0.05; ** p = < 0.01; *** p < 0.001. Abbreviations: ns: not (statistically) significant; TM: tetramer.

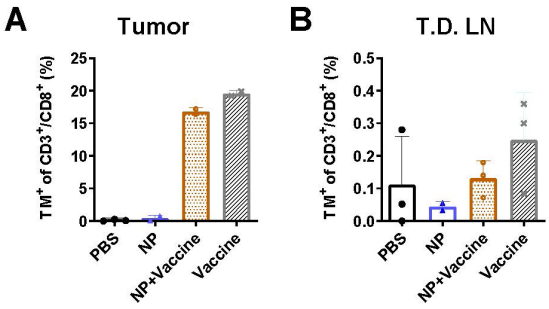

Figure S5. Cancer antigen-specific T cells in the tumor and the tumor-draining lymph node

Quantification of CD3+CD8+TM+ specific T cells in specified organs at day 20 after mock treatment (PBS), vaccination only, intratumoral injection with NP(pIC+R848+MIP3α) only, or combined vaccination and intratumoral injection with NP(pIC+R848+MIP3α). A) The levels of CD3+CD8+TM+ T cells in the tumor. B) The levels of CD3+CD8+TM+ T cells in the tumor-draining lymph node. Abbreviations: NP: NP(pIC+R848+MIP3α); TM: tetramer.

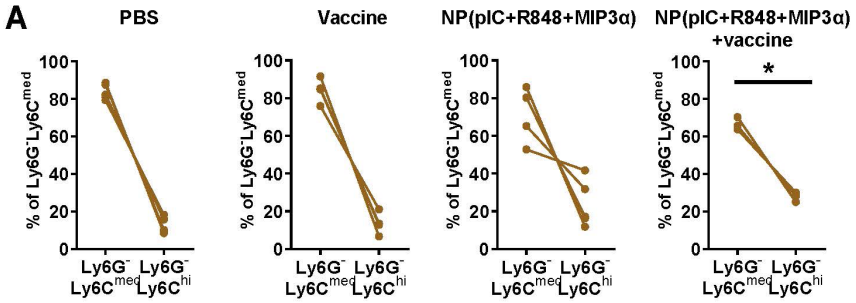

Figure S6. Macrophage population phenotype shift in the tumor-draining lymph node upon treatment with immunomodulators

Shown are the Ly6G-Ly6Cmed (suppressor tumor-associated macrophages) and the Ly6G-Ly6Chi (inflammatory monocytes) gated from CD11b+F4/80+ gate from the tumor-draining lymph node in mice treated as per described: PBS vs. vaccine, p=0.9048; PBS vs. NP(pIC+R848+MIP3α), p=0.0952; PBS vs. vaccine plus NP(pIC+R848+MIP3α), p=0.0357. Statistics were calculated using a two-tailed Mann Whitney test. Statistical differences were considered significant at * p = < 0.05; ** p = < 0.01; *** p < 0.001.